Journal of Engineering and Development, Vol. 18, No.5, September 2014, ISSN 1813- 7822

First Diagonal Cracking and Ultimate Shear of Reactive Powder Concrete T-Beams without Stirrups

Prof. Dr. Hisham Mohamad Ali
Building and Construction Department, University of Technology

Asst. Prof. Dr. Jamal* Saeed *abd alamir
civil Engineering College, Al-Mustansiriyah University

Lecturer. Nagham Tariq Hamad
Highway & Transportation Engineering Department, Al-Mustansiriyah University

Abstract

The first diagonal cracking and ultimate shear load of reactive powder concrete (RPC) T-beams were investigated in this paper. Six beams were tested, a simplified formulation for the first diagonal cracking capacity V_{cr} is proposed while the analytical model to predict the ultimate shear capacity V_u is formulated based on the two bounds theory (upper and lower bound). A fiber reinforcing parameter is constituted and used based on the Variable Engagement Model (VEM). The predicted values of V_{cr} and V_u are compared with the test results and gives good agreements.

Keywords: first diagonal cracking and ultimate shear load, Reactive Powder Concrete& Tee Beams

التشققات القطرية الأولى والقص الأقصى لعتبات خرسانة المساحيق الفعالة ذات مقطع –T والخالية من الاتاري

أ.د.هشام محمد علي
قسم هندسة البناء والإنشاءات
الجامعة التكنولوجية

أ.م.د. جمال سعيد عبد الامير
قسم الهندسة المدنية
الجامعة المستنصرية

م. نغم طارق حمد
قسم هندسة الطرق والنقل
الجامعة المستنصرية

الخلاصة :

في هذا البحث،تم استقصاء اول حمل للتشقق القطري والتحمل الاقصى للقص لخرسانة المساحيق الفعالة ذات المقطع - T. تم اختبار ستة عتبات، وقد تم اقتراح صيغة مبسطة لحمل التشقق V_{cr} في حين تم اشتقاق سعة القص القصوى V_u سوية مع قوة القصّ المتصدّعة باستخدام نموذج مستند على نظريات الحدّ الاعلى والحد الادنى للدونة.ان تشكيل واستخدام الالياف الفولاذية استند الى نموذج ترابط المتغيرات (VEM)).وقد تم مقارنة القيم المتوقعة لكل من (V_{cr} و V_u) مع نتائج الاختبارو اعطت النتائج توافق جيد.

1. Introduction

Reactive powder concrete (RPC) is a cementitious material that exhibits high-performance properties such as limited shrinkage and creep, low permeability, ultra-high strength and increased protection against corrosion. The properties of RPC make it a revolutionary material in the field of concrete technology with possibilities for use in a wide range of structural and non-structural applications[1]. RPC is characterized by high strength and very low porosity, which is obtained by optimized particle packing and low water content. It has capacity to deform and support flexural and tensile loads, even after initial cracking. The durability properties are those of an impermeable material, there is almost no penetration of chlorides and sulphates and high resistance to sulphate attack. Resistance to abrasion is similar to that of rock. The development of RPC has the potential to revolutionize design in precast, prestressed, concrete[1]. Currently, to achieve excellent mechanical behavior, some special techniques and raw materials must be adopted in the preparation of ultra high performance concrete(UHPC), which include:

a. Coarse aggregate is removed to enhance the homogeneity of concrete.
b. Metal fiber or steel tube is introduced to improve ductility of composites.
c. High quality superplasticizer and large quantities of superfine silica fume and quartz are added to achieve a low water/binder ratio to reduce porosity and improve strength.
d. Pressure may be applied before and during the setting to increase the compactness of the concrete.
e. High activity micro-silica and/or precipitated silica may be mixed into cementitious materials to accelerate the hydration of cement and catalyze a strong pozzolanic reaction effect.
f. Steam curing may be supplied to gain higher strength.

2. Specimen Dimensions

The experimental program included casting and testing six RPC T-beams without steel stirrups. The specimens were designed to fail by diagonal tension (shear) in the web region.

All tested beams were simply supported and subjected to two point loads **Figure.(1).** Each beam had 1300 mm total length and 1200 mm span between the supports. The beam dimensions and details are shown in **Figure. (1)** and **Table (1).**

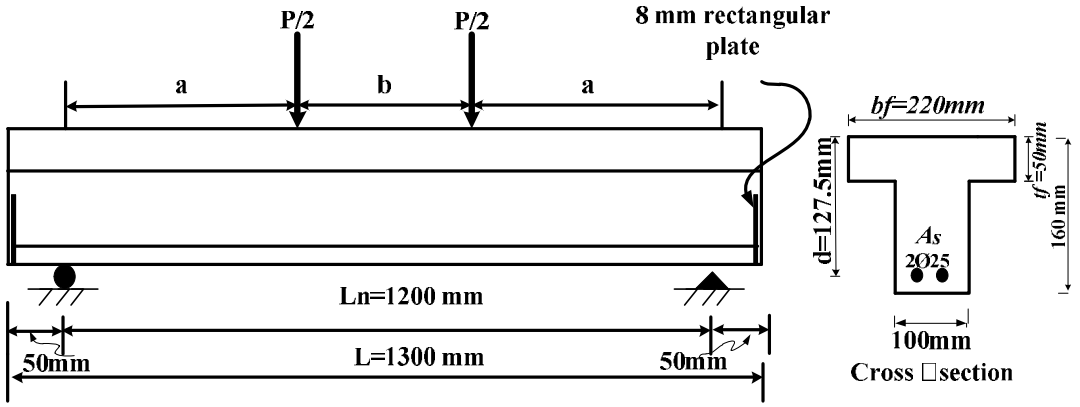

Fig .(1) Details of a Typical Test Beam.

Table .(1) Beam groups and Concrete Properties.

Group	Beam No.	V_f%	a/d	SF%	$\rho_w = (A_s/b_w d)$%
Change in V_f	2	1	3.5	25	7.7
	3	2	3.5	25	7.7
Change in a/d	3	2	3.5	25	7.7
	4	2	2.5	25	7.7
	5	2	4.3	25	7.7
Change in SF	3	2	3.5	25	7.7
	6	2	3.5	20	7.7
	7	2	3.5	15	7.7

3. Material, Mix Design and Fabrication

Details of the RPC mixes for specimens B2 to B7 are given in **Table 2**. The cement used in this paper was Tasluoja Ordinary Portland cement Type 1. General Portland cement used conformed to the Iraqi specification No.5 / 1984. [2]

The silica fume used was with particle size range between 150 μm and 400 μm. The superplasticizer used in the mix was Flocrete PC 260, which is a polycarboxylic ether based superplasticizer. The fibers were straight 13 mm long by 0.2 mm diameter and are fabricated from very high strength steel with minimum tensile strength of 1800 MPa. two fiber volume ratios (V_f) were used 1 and 2 %.

The mix type M1,25 was adopted as a reference mix which had 1% steel fibers and 25% silica fume ratio. The four types of RPC mixes of **Table (2)** were used to cast the main beam specimens in the present investigation as well as their control specimens.

All the dry components (i.e. cement, silica fume and sand) were pre-batched into 0.5 tone bags. The dry components were then transported to the high energy mixer and mixed for

about 10 minutes. Water and superplasticizer were added gradually until the materials were uniformly mixed. The fibers were introduced last, dispersed uniformly and mixing continued for a further 2-3 minutes. All specimens were cast vertically in steel forms as shown in **Plate 1**. The molds were cleaned and greased to allow smooth stripping. The fresh RPC was compacted using external vibrators which were attached to the steel molds. Within one hour of casting, the specimens and test control samples were covered under plastic nylon until the day of demoulding. After stripping at age 1 days, the specimens were cured for 2 days at 80°C in a hot water bath. At age 3 days the specimens were removed from the hot water bath and stored in water at 25°-30° C for 28 days then stored in the laboratory until the time of testing.

Table .(2) Properties of the Different Types of RPC Mixes

Mix Type	Beam No.	Cement kg/m3	Sand kg/m3	Silica fume* %	Silica fume kg/m3	w/c	Flocrete PC 260**%	Steel fiber content*** %	Steel fiber content kg/m3
M1,25	B2	1000	1000	25	250	0.2	3.0	1	78
M2,25	B3,B4,B5	1000	1000	25	250	0.2	3.0	2	156
M2,15	B7	1000	1000	15	150	0.2	3.0	2	156
M2,20	B6	1000	1000	20	200	0.2	3.0	2	156

* Percent of cement weight.

** Percent of binder (cement + silica fume) weight.

*** Percent of mix volume**.**

Plate (1) casting and curing of specimens

4. Test Setup and Instrumentation

All beams and control specimens were removed from the curing water tank at age of 28 days. Before testing, the beam was cleaned and painted white to allow easy detection of crack propagation. The demec points were placed in different position on the beam. The beam was placed on its supports in the machine with a clear span of 1200 mm. Loading was applied through steel plates to avoid stress concentration on the beam flange. The test of the RPC T-beam is shown in **Plate (2).**

All beams were tested under two points loading. The dial gage was placed in its position touching the bottom surface of the beam at mid-span. Before loading was applied, the zero-load readings of the mechanical strain gages as well as the dial gage were taken and then a load of 5 kN was applied and released in order to recheck the zero-load readings.

The magnitude of the load at every single step of loading was chosen according to the expected strength of the beam. At each load value, concrete surface strains reading was recorded and a search was made for the appearance of the cracks by using a magnifying glass. The positions and extents of the first and the other consequent cracks were marked on the surface of the beam and the magnitude of the applied load at which these cracks occurred was written. The inclined cracking load was reported as being the load causing the critical diagonal crack to cross the mid-depth of the beam. The beam was considered to reach failure when it showed a drop in loading with increasing deformation. The failure load was thus recorded, and the load was then removed to allow taking some photographs of the final crack pattern.

Plate (2) Testing RPC T-Beam

5. Mechanical properties

The results of the material control tests are summarized in **Table 3** the mean compressive strength (f'_{cf}) was determined from six 200 mm high by 100 mm diameter cylinders stressed under load control at a rate of 20 MPa per minute. The ends of the cylinders were ground flat. The modulus of elasticity (E_o) was obtained from stress-strain tests on 200 mm high by 100 mm diameter cylinders The tensile strength of the material was evaluated using split cylinder (Brazil) tests. The split cylinder tensile strength (fsp_f) was obtained from tests on six 200 mm high by 100 mm diameter cylinders loaded at 1.0 MPa per minute via a 10 mm wide loading strip. The two point flexural tension strength (f_{rf}) was obtained from 100 mm square prisms spanning 500 mm to find modulus of rupture (f_{rf}). As show in **plate (3)**

Plate .(3) Modulus of Elasticity (E_o), Modulus of Rupture and Compressive Strength (f'_{cf}) Tests

Table .(3) Properties of Hardened RPC.

Type of mix	Fiber content (V_f)%	Silica Fume SF%	Compressive Strength *f'cf* (MPa)	Splitting Tensile Strength *fspf* (MPa)	Modulus of Rupture *frf* (MPa)	Modulus of Elasticity *Ec* (GPa)
M1,25	1	25	127	14.7	15.3	50.52
M2,25	2.	25	148	19.8	21	54.72
M2, 20	2	20	139	17.3	19	52.90
M2,15	2	15	130	16.4	18.6	51.13

6. Test results and observations

The experimental results of the shear tests are summarized in **Table 4** where *Vcr* is the force at which the first shear cracking was detected visually on the specimen and *Vu* is the maximum force recorded during the experiments.

Table .(4) Details of Cracking and Ultimate Shear Strength for Test Beams

beams	V_f %	ρ_w	SF %	*a/d*	f'_{cf} (MPa)	Shear strength (kN)		$\frac{V_{u,test}}{V_{cr,test}}$	Mode of failure*
						V_{cr}	V_u		
B2	1	0.077	25	3.5	127.0	30.0	70.50	2.35	DT
B3	2	0.077	25	3.5	148.5	40.0	122.75	3.07	DT
B4	2	0.077	25	2.5	148.5	45.0	209.5	4.66	DT
B5	2	0.077	25	4.3	148.5	30.0	100.0	3.33	DT
B6	2	0.077	20	3.5	139.0	37.5	119.25	3.18	DT
B7	2	0.077	15	3.5	130.0	35.0	111.5	3.19	DT

Diagonal tension failure

7. Plastic Shear Model

The plastic shear model (PSM) is used to calculate the ultimate shear strength V_u of the RPC T-beams that do not contain shear reinforcement. This model is based on the theorem of plasticity in concrete, which was pioneered by Nielsen [3] and subsequently developed by Zhang (1994) [4] and Hoang (1997) [5].

In applying the theory of plasticity to concrete structural elements, reinforcement is assumed to resist forces in axial direction only, with yield stress equal to f_y . Concrete is assumed to behave as a rigid, perfectly plastic material, obeying the modified Coulomb failure criterion with the associated flow rule (Nielsen 1999) [6].

At failure, the cracked concrete in compression is simultaneously subjected to compression and tensile strains with the tensile strain occurring in a direction orthogonal to compression strains. Therefore, it exhibits a reduced strength compared to the uncracked concrete in uniaxially compression. This physical behavior is called compression softening and can be recognized in the plastic theory by the effectiveness factors for concrete.

For fibrous concrete beams, the flattened stress-strain relationships in the post peak range in compression and tension make the application of the plastic theory more suitable than plain concrete. Moreover, the presence of fibers in the matrix induces the reduction of slips along cracks. To apply the plastic theory to fibrous concrete beams, the most important issue is the use of reliable constitutive laws for fibrous concrete.

The residual tensile stress of SFRC (steel fiber reinforced concrete) also plays a key role in the shear failure mechanism of the beam, especially for slender structural elements. The analytical relationship proposed by (Foster et al. 2006) [7], namely the variable engagement model (VEM06), for fibrous concrete in direct tension is adapted to evaluate the effective tensile strength ($f_t^* = \nu_t \cdot f_{tf}$). The VEM06 considers that slip between fibers and concrete matrix occurs before the full bond stress is developed, and the fibers fracture themselves before being pulled out across a crack.

$$f_{tf} = K_{f,max}\,\alpha_f\,V_f\,\tau_b \qquad \text{.....(1)}$$

where $\alpha_f = l_f / d_f$ is the aspect ratio of the fiber, V_f was the volumetric fraction of fibers, τ_b is the bond stress between the fibers and the concrete matrix and $K_{f,max}$ is the maximum value of global orientation factor.

the maximum value of the global orientation factor, $K_{f,\,max}$, can be obtained as:

$$K_{f,max} = 0.5 - \frac{0.645}{\alpha_f^{0.45}} \qquad \text{.....(2)}$$

In the formulation of Eq. (2), it was assumed that all fibers were pulled out from the matrix and there was no fiber fracture.

The VEM model adopted here is based on a uniform bond model, then, the interfacial fiber/matrix bond strength for UHPC is taken as:

$$\tau_b = 0.6\sqrt{f'_{cf}} \ldots\ldots\ldots (for\ straight\ fibers) \qquad \text{.....(3)}$$

8. Ultimate Shear Capacity V_u of RPC T-Beams. (Upper Bound Solution).

Upper bound plasticity approach can be used to calculate the ultimate shear capacity V_u of RPC T-beams. Hoang [5] has previously modeled the shear strength of simply supported ordinary RC T-beams without shear reinforcement under concentrated loading. Hoang's model for the ordinary RC T-beam is modified in this research to incorporate RPC T-beams.

The experimental tests of the RPC T-beams of the present study showed that the general failure mechanism of an RPC T-beam without stirrups is similar to the failure mechanism of a normal concrete T-beam without stirrups. That is, the failure mechanism consists of a sliding failure along a crack in the web and rotation of the hinges in the compression flange, see **Figure. (2)** and **Plate (4).**

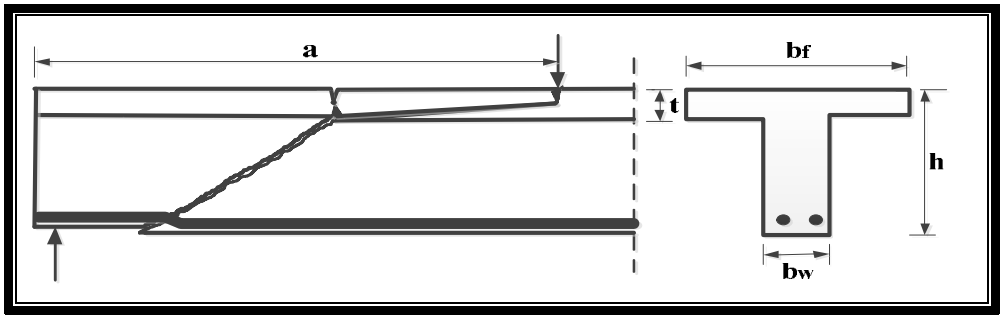

Fig .(2): Shear Failure Mechanism of Simply Supported Ordinary R.C T-Beam (Hoang, 1997) [5].

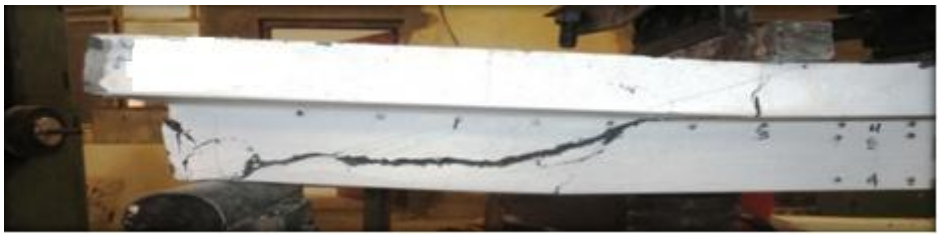

Plate .(4): Shear Failure Mechanism of Simply Supported in RPC T- Beam.

The complexity of **Hoang**'s model makes it less suitable as a general design tool. Therefore**,** a more simplified model is proposed here to calculate the ultimate shear capacity *Vu* considering the sliding failure mechanism of the virtual crack yielding line shown in **Figure. (3).**

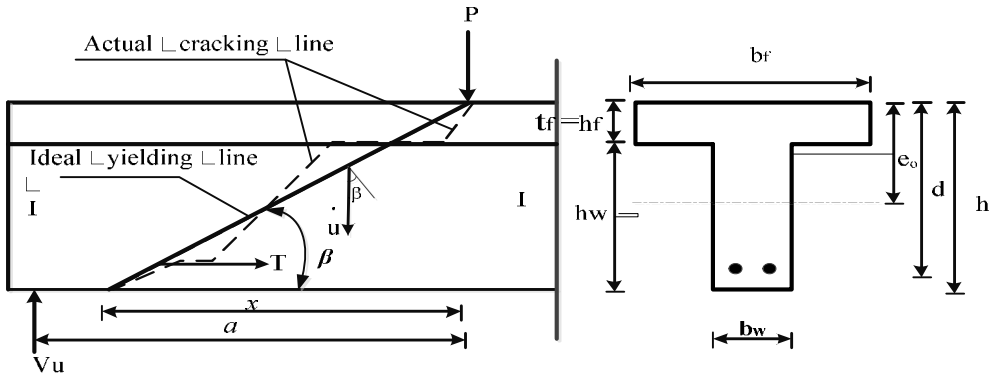

Fig .(3) The Proposed RPC T-Beam Shear Model.

The work equation may be written in the form

$$W_E = W_{I,web} + W_{I,flange} \qquad \text{.....(4)}$$

where $W_{I,web}$ and $W_{I,flange}$ are the internal work represented by the contributions of the web and the flange, respectively. W_E is the external work given as

$$W_E = V_u \cdot u \qquad \text{.....(5)}$$

where u is the relative displacement.

Based on the plane stress limit analysis of concrete plasticity the internal work W_I along the cracking surface can be simplified as

$$W_I = 0.5\, f_c^* u\, b[1 - \cos\beta]\frac{h}{\sin\beta} \qquad \text{.....(6)}$$

in which , β is the angle between the ideal line and the horizontal axis as shown in Fig. (3). f_c^* is the effective concrete strength, which is taken as

$$f_c^* = \nu_c f'_{cf} \qquad \text{.....(7)}$$

with the compression effectiveness factor is taken as $\nu_c = 0.8$ [7].

$$\cos\beta = \frac{x}{\sqrt{x^2 + h^2}} \qquad \text{.....(8)}$$

Based on Eq. (6), the virtual work equation (4) along cracking surface becomes

$$W_{E(web+flange)} = \frac{0.5\, f_c^* u(1-\cos\beta)}{\sin\beta}\left[b_w h_w + b_f t_f\right] \qquad \text{.....(9)}$$

Since $[b_w\, h_w + b_f t_f]$ represents the gross area A_c of the beam T-section, thus:

$$W_E = 0.5\, f_c^*.u\left(\frac{1-\cos\beta}{\sin\beta}\right) A_c \qquad \text{..... (10)}$$

From Eqs. (5) and (10), the ultimate shear capacity ***Vu*** can be

$$V_u = 0.5\, f_c^*\left(\frac{1-\cos\beta}{\sin\beta}\right) A_c \qquad \text{..... (11)}$$

Substituting Eq. (8) in Eq. (11) gives

$$V_u = 0.5\, f_c^* A_c \left[\sqrt{1+\left(\frac{x}{h}\right)^2} - \frac{x}{h}\right]$$

and by replacing 0.8 $f_{cf}^{'}$ for f_c^* as indicated by Eq.(7), the ultimate shear capacity of RPC T-beams (V_u) becomes:

$$V_u = 0.4\, f_{cf}^{'} A_c \left[\sqrt{1+\left(\frac{x}{h}\right)^2} - \frac{x}{h}\right] \qquad \text{..... (12)}$$

9. Cracking Shear Force V_{cr} (Low Bound Solution).

First cracking Shear Force V_{cr} for RPC T-beam is found by calculating the moment at the upper tip of the crack in **Figure. (4).** Diagonal crack is initiated once the first principal stress σ_1 of yield line exceeds the tensile strength of RPC f_{tf}, and the crack is perpendicular to the direction of σ_1. In the shear/bending area, the direction of σ_1 is variable due to the combination of shear stress and normal stress, and the crack is curved but can be assumed linear for simplicity of analysis. A fully developed diagonal crack is illustrated in **Figure. (4).**

In the case of a critical diagonal crack, the crack is supposed to be fully developed. Thus a fully plastic equivalent stress distribution may be assumed, i.e. the tensile stress along the path of crack, perpendicular to the crack, is distributed evenly with the value of f_t^* shown in **Figure. (4).** This assumption is similar to that of a flexural crack. At ultimate state, the depth of the compressive zone becomes very small. Neglecting this zone, the upper tip of the diagonal crack is assumed to be at point B of the top surface as shown in **Figure. (4).** The direction of the tensile stress is perpendicular to the crack path. Therefore, the internal moment along the original crack with respect to point **B** is the same as that along the straight line AB. Here, ***T*** is the equivalent tensile force of the reinforcing steel bars. Aggregate

interlock action can be ignored for fine aggregate condition. Two segments (1) and (2) are considered for the moment analysis of the distributed tensile stress as can be seen in Fig. (4). d is the effective depth of the section and $e_\circ$ denotes the distance from the top face of the flange to the centroid of the gross area of the T-section.

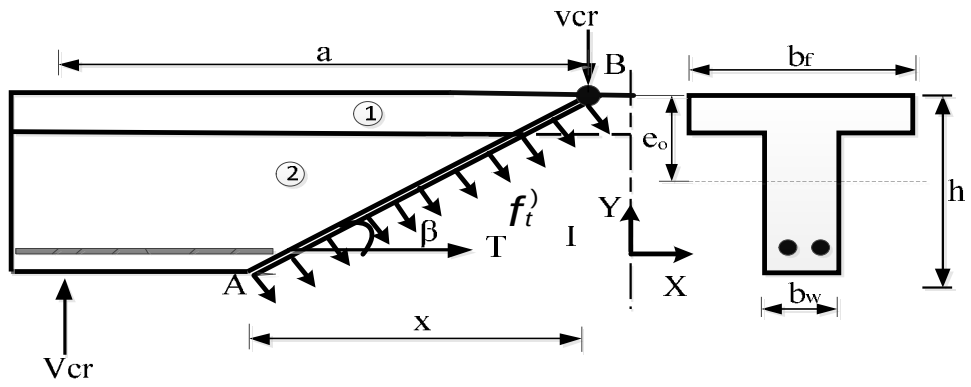

Fig .(4) Stress Distribution along the Critical Diagonal Crack for RPC T-Beams.

Equilibrium analysis

$$\sum M_B = 0 \ \curvearrowleft$$

$$f_t^* A_c e_\circ \left[\left(\frac{x}{h}\right)^2 + 1\right] + T.d - V_{cr}.a = 0 \qquad \text{..... (13)}$$

$$V_{cr} = \frac{f_t^* A_c \ e_\circ \left[\left(\frac{x}{h}\right)^2 + 1\right] + T.d}{a} \qquad \text{.....(14)}$$

where T is the tensile force of the steel reinforcement ($T = As\ f_y$), f_y is the yield stress of the steel bars and f_t^* is the effective plastic tensile strengths of the FR composite [7] which is taken as:

$$f_t^* = \nu_t f_{tf} \qquad \text{..... (15)}$$

with the tensile effectiveness factor taken as $\nu_t = 0.8$ and where f_{tf} is the maximum stress of the fiber component according to the VEM. Ac is the gross area of the T-beam section and $e_\circ$ is the distance from the top face of the flange to the centroid of Ac as given below; $e_\circ$ is given as:

$$e_\circ = \frac{1}{2}\frac{\left(b_w h^2 + (b_f - b_w) t_f^2\right)}{A_c} \qquad \text{..... (16)}$$

10. Solution of *x* and Shear Force Capacity.

The intersection of the two bounds V_u and V_{cr}, which can be solved by iteration method, determines both the position of the limit yield line and the shear force carrying capacity. Equating Eqs.(12) and (14) gives;

$$\mathbf{0.4}\, f'_{cf}\left[\sqrt{1+\left(\frac{x}{h}\right)^2}-\frac{x}{h}\right]=\frac{f_t^{*}\, e_{\circ}\left[\left(\frac{x}{h}\right)^2+1\right]}{a}+\frac{T\,.d}{a\,.A_c} \qquad \text{..... (17)}$$

The shear capacity $\boldsymbol{V_u}$ is then determined by Eq. (12).

11. Proposed Simple Formula For The Cracking Shear Force *Vcr*

Based on regression analysis of the results obtained from the experimental tests carried out in the present research on RPC T-beams, a simple formula is proposed for estimating the cracking shear force V_{cr} for such beams as given below.

$$V_{cr}=\frac{2.54\, V_f^{0.2}\,.\left(\frac{a}{d}\right)}{\left[\left(0.5\,\frac{a}{d}\right)^{1.05}\left(52.3+15.6\,\frac{a}{d}\right)\right]}\left(\frac{b_w}{d}\right)^{3.9} f'_{cf}\, b_w d \qquad \text{.....(18)}$$

In which, $\boldsymbol{V_f}$ is the fiber volume fraction, $\boldsymbol{a/d}$ is the shear span to depth ratio, $\boldsymbol{d}$ is the effective depth of the beam, $\boldsymbol{f'_{cf}}$ is the compressive strength of RPC and $\boldsymbol{b_w}$ is the beam web width.

12. Numerical Calculations and Comparative Analysis.

The cracking and ultimate shear strength ($\boldsymbol{V_u}$ and $\boldsymbol{V_{cr}}$) calculated using the plasticity model described above for the RPC T- beams tested in this study are compared with the corresponding values obtained experimentally as presented in **Table (5).** The theoretical predictions of $\boldsymbol{V_u}$ and $\boldsymbol{V_{cr}}$ are based on the two bound theorems of plasticity (the lower bound theorem and upper bound theorem respectively) are shown in **Figure. (5)**

Comparing the results of the plastic design model with the corresponding experimental values shows that the plastic model presented provide reasonable correlation with the actual shear strength obtained from test with the mean experimental to theoretical ratios of 0.94 with coefficients of variation 13.6% as shown in **Figure.(6).** The Proposed $\boldsymbol{V_{cr}}$ equation gives good agreement with the test results as shown in **Figure. (7).** It can also be noticed that $\boldsymbol{V_{cr}}$ is 30% ~ 60% of $\boldsymbol{V_u}$, which implies that $\boldsymbol{V_{cr}}$ has a key significance for RPC T-beams. The two limits division is necessary since the gap was in between $\boldsymbol{V_{cr}}$ and $\boldsymbol{V_u}$. Thus, a strength reduction factor 0.85 is proposed here for safety measures.

Table .(5) Comparison of Plasticity Based Shear Capacity V_{cr} and Vu (for RPC T- Beams) with Test Results.

Beam No.	f'_{cf} (MPa)	V_{cr} (kN) (Eq.)		$\frac{Vcr\ test}{Vcr\ predict}$	V_u (kN) (Eq.)		$\frac{Vu,test}{Vu,theo.}$
		V_{cr}-test	V_{cr}-prediction		Vu-test	Vu- theo.	
B2	127	30	28.9	1.03	70.50	82.0	0.86
B3	148.5	40	38.9	1.03	122.24	121.6	1.00
B4	148.5	45	46.3	0.97	209.5	172.2	1.20
B5	148.5	30	34.4	0.87	100.0	107.0	0.93
B6	148.5	42	42.2	0.99	134.0	135.0	0.99
B7	148.5	45	44.8	1.00	145.0	146.6	0.98
Average				1.00			0.95
COV.				2.4%			13.6%

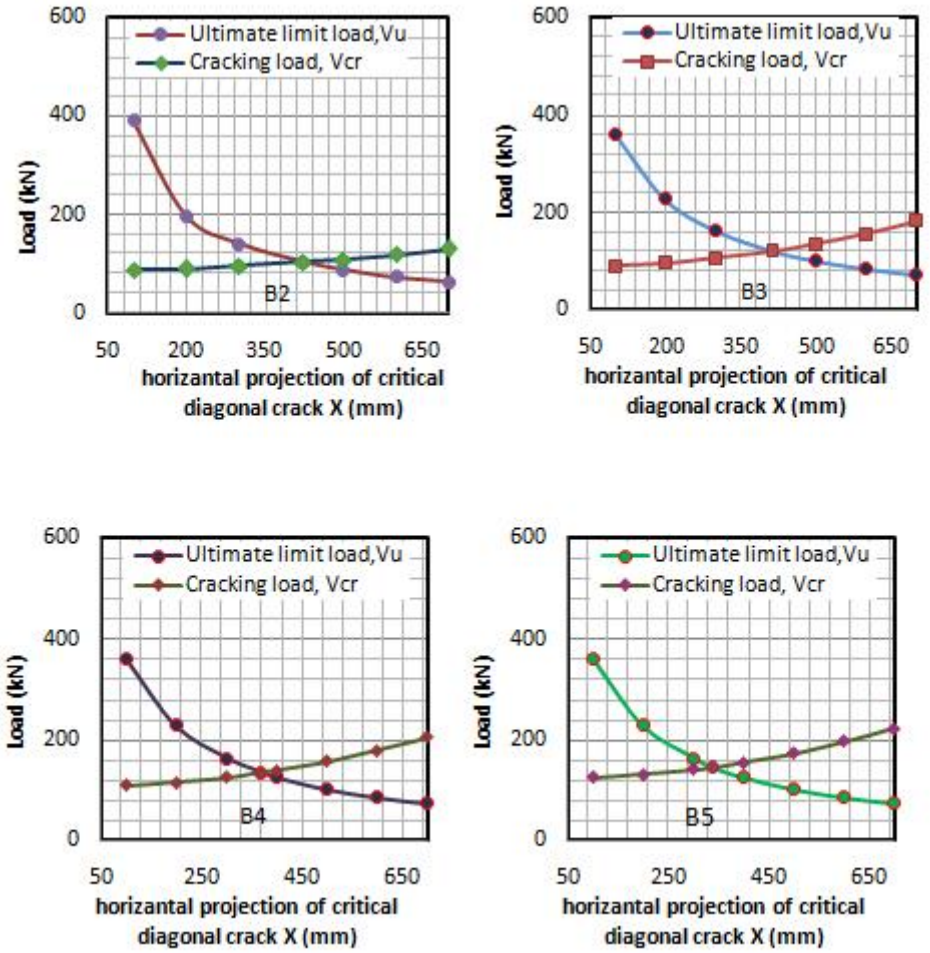

Fig .(5): Variation of the Two Bounds with Crack Projection Length (X)

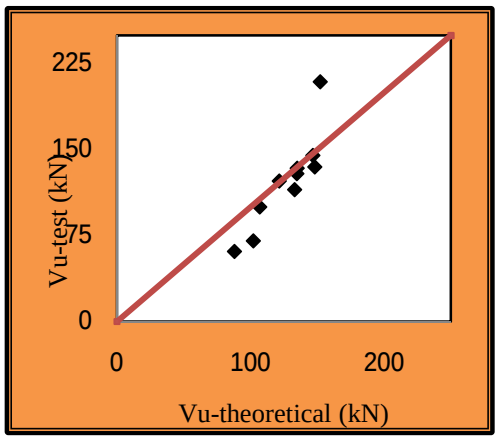

Fig .(6) Tests Values Versus Theoretical Values of Ultimate Shear Capacity (V_u)

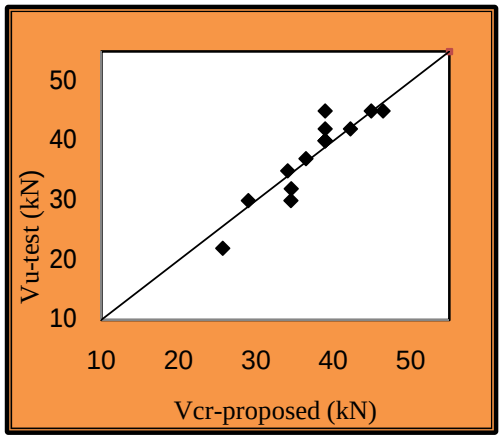

Fig .(7) Tests Values Versus Proposed Values of cracking Shear Force (V_{cr}).

13. Conclusions

1. The result of compression on RPC cylinders indicate that increasing the steel fibers volumetric ratio V_f and/or silica fume SF increase the compressive strength (f'_{cf}) of RPC. For the mixes used in this research, the highest compressive strength (f'_{cf}) was 148.5 MPa which was recorded for V_f = 2% and SF = 25%.
2. It was found that the addition of steel fibers to RPC mixes resulted in a higher improvement of splitting tensile strength than of compressive strength.
3. Increasing steel fibers ratio from 1 to 2% increases modulus of rupture by 303.85% while increasing silica fume content from 15 to 25% increases modulus of rupture by only 12.9%. Straight steel fibers increase tensile strength of concrete by arresting micro cracks.
4. The quantity of fibers used in the concrete mixture did not significantly affect the cracking load of RPC T-beams but had a significant influence on the rate of crack propagation and on the value of the failure load.
5. At the peak load, many fine cracks had formed in the web, with the cracks well distributed through the shear spans. The failure loads of RPC T-beams, were more than twice the cracking loads.
6. Decreasing the silica fume content SF from 25% to 20% and 15%, in RPC T-beams decreased the diagonal cracking load by 6.25% and 12.5% respectively and the ultimate load by 3% and 9.2% respectively.
7. Increasing the silica fume content SF from 15% to 20% and 25% in RPC T-beams having V_f= 2% showed a lesser maximum crack width at a specific load level beyond the cracking load.

8. Increasing the shear span to effective depth ratio a/d from 2.5 to 3.5 and 4.5 in RPC T-beams having V_f= 2% and ρ_w = 7.7%decreased both diagonal crack load by 11.11% and 33.33% respectively and the ultimate load by 41.4% and 52.3% respectively.
9. The equation derived for the predication of the cracking shear force V_{cr} and ultimate shear capacity (***Vu***) based respectively on the lower bound and upper bound theorems of plasticity showed reasonable estimates of the shear capacities of the RPC T-beams.

14. Reference

1. **Bonneau, O., Poulin, C., Dugat, J., Richard, P., and Aitcin, "Reactive Powder Concretes: From Theory to Practice", Concrete International, Vol. 18, No. 4, April 1999, pp. 37-39.**
2. **Iraqi Specification, No. 5/1984., "Portland cement".**
   وزارة التخطيط ،الجهاز المركزي للتقييس والسيطرة النوعية.
3. **Nielsen, M.P., "Om forskydningsarmering i jernbetonbjælker- On Shear Reinforcement in Reinforced Concrete Beams", Bygninsstatiske Meddelelser, Vol. 38, No. 2, November 1967, pp: 33-58.**
4. **Zhang, J.P., "Strength of Cracked Concrete: Part 1 – Shear Strength of Conventional Reinforced Concrete Beams, Deep Beams, Corbels, and Prestressed Reinforced Concrete Beams without Shear Reinforcement", Report No. 311, Technical University of Denmark, Department of Structural Engineering, Lyngby, (1994), 106 pp.**
5. **Hoang, L. C., "Shear Strengths of Non-Shear Reinforced Concrete Elements, Part 2 –T-Beams", Technical University of Denmark, Department of Structural Engineering and Materials, Report No. 29, Lyngby, 1997, 35 pp.**
6. **Nielsen, M. P., "Limit Analysis and Concrete Plasticity", 2nd Ed., CRC, Boca Raton, Fla.**
7. **Foster, S. J., Voo, Y. L., and Chong, K. T., "FE Analysis of Steel Fiber Reinforced Concrete Beams Failing in Shear: Variable Engagement Model", ACI SP-237, Detroit, 2006, pp. 55–70.**

Appendix

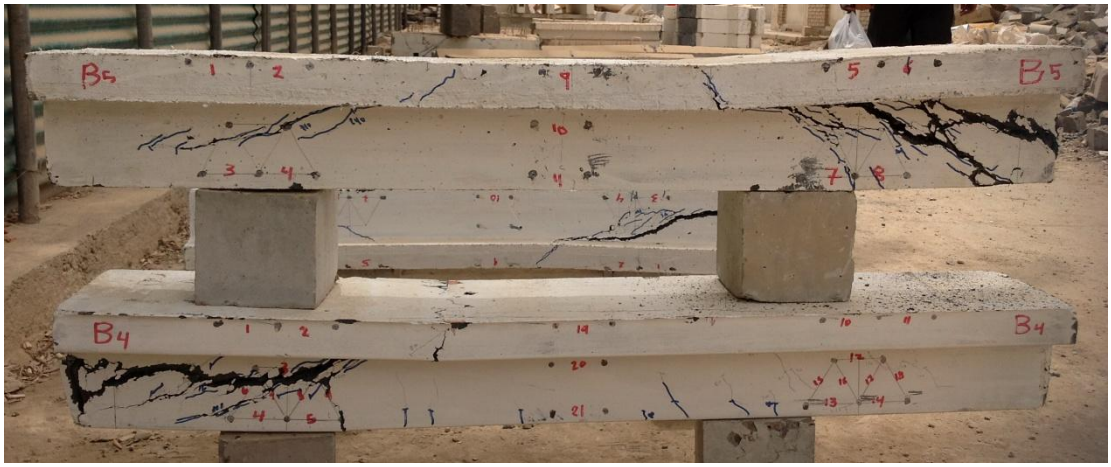

Plate Crack Patterns for Fibrous T- Beams